

Quantized magneto-thermopower in tunnel-coupled ballistic channels: sign reversal and oscillations

This article has been downloaded from IOPscience. Please scroll down to see the full text article.

2004 J. Phys.: Condens. Matter 16 3379

(<http://iopscience.iop.org/0953-8984/16/20/009>)

View [the table of contents for this issue](#), or go to the [journal homepage](#) for more

Download details:

IP Address: 129.252.86.83

The article was downloaded on 27/05/2010 at 14:39

Please note that [terms and conditions apply](#).

Quantized magneto-thermopower in tunnel-coupled ballistic channels: sign reversal and oscillations

S K Lyo¹ and D H Huang²

¹ Sandia National Laboratories, Albuquerque, NM 87185, USA

² Air Force Research Laboratory (AFRL/VSSS), Kirtland Air Force Base, NM 87117, USA

Received 27 February 2004

Published 7 May 2004

Online at stacks.iop.org/JPhysCM/16/3379

DOI: 10.1088/0953-8984/16/20/009

Abstract

The quantized electron-diffusion thermoelectric power S is studied for a general one-dimensional band structure in ballistic channels with applications to a single-quantum-well channel and tunnel-coupled double-quantum-well channels in a perpendicular magnetic field. We find a field-induced sign reversal of S and oscillations in double-well channels.

Transport properties of quasi-one-dimensional (1D) doped semiconductor structures are of current interest. An earliest form of 1D single-quantum-well wires (SQWRs) is the so-called quantum point contact illustrated in figure 1(a), where the channel length is very short, of the order of a fraction of a micrometre. Electrons pass through this wire (or channel) ballistically at low temperatures (T) under a DC bias. The conductance G is quantized and decreases in steps of $2e^2/h$ in a spin-degenerate system (assumed in this paper) when the channel width is reduced gradually [1]. Here, e is the absolute electronic charge and h is Planck's constant. Similar quantized G steps were observed in SQWRs as a function of a magnetic field B applied in the perpendicular (i.e., z) direction shown in figure 1(a) [2]. Recently, ballistic thermoelectric power (TEP) S was observed in SQWRs [3] and was also studied theoretically in zero B [3–5]. Previous studies of the TEP [3–5] are relevant to simple band structures with a single minimum for each sublevel. More complicated band structures with two minima and a maximum are generated in tunnel-coupled double-quantum-well wires (DQWRs) in the presence of a perpendicular B as shown in figure 1(b) [6, 7]. For simplicity, we assume that the wells are narrow and deep in the growth (z) direction, allowing only the ground-level occupation. However, channels may be wide in the x direction and allow multi-sublevel occupation. In this paper, we calculate the ballistic electron-diffusion TEP for a general 1D structure and apply the result to SQWRs and DQWRs in perpendicular B . We find that in ballistic DQWRs B causes a sign reversal of S and oscillations.

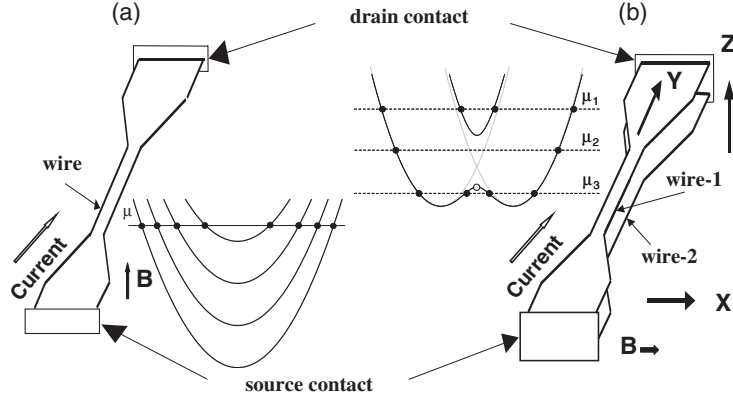


Figure 1. (a) A schematic diagram of a SQWR and the energy dispersion. A narrow channel is formed by applying a negative bias on the top split metallic gate, not shown. (b) A schematic diagram for DQWRs and the energy dispersion in a magnetic field. Electrons tunnel between the wires through the $\text{Al}_x\text{Ga}_{1-x}\text{As}$ barrier in the z direction. Electrons behave like holes for the TEP at the hollow circle on the dispersion curve. A magnetic field B lies in the x direction for the DQWRs and in the z direction for the SQWR. Black dots denote the Fermi points.

The electron-diffusion TEP is the ratio of the heat current and the charge current of the electrons divided by T in the presence of a linear DC field. The ballistic heat ($Q^{(1)}$) and charge ($Q^{(0)}$) currents are given, for symmetric electronic structures, by

$$Q^{(\ell)} = 2(-e)^{1-\ell} \sum_{n,k} \frac{v_{nk}}{\mathcal{L}} (\varepsilon_{nk} - \bar{\mu})^\ell [\theta(-v_{nk}) f_{nk,R}^{(0)} (1 - f_{nk,L}^{(0)}) + \theta(v_{nk}) f_{nk,L}^{(0)} (1 - f_{nk,R}^{(0)})], \quad (1)$$

where $\ell = 0, 1$, \mathcal{L} is the channel length, $\bar{\mu}$ is the chemical potential in the channel, and $\theta(x)$ is the unit step function. In equation (1), n is the sublevel index, k is the wavenumber, $v_{nk} = \partial\varepsilon_{nk}/\partial\hbar k$ is the velocity, and $f_{nk,\alpha}^{(0)}$ is the Fermi function for the 2D electron gas (2DEG) on the left- ($\alpha = L$) and the right-hand ($\alpha = R$) side, with the chemical potential μ_α . The physical meaning of equation (1) is self-evident. Equation (1) can be simplified, in view of $v_{n,-k} = -v_{nk}$, as

$$Q^{(\ell)} = \frac{2(-e)^{1-\ell}}{\pi} \sum_n \int_0^\infty |v_{nk}| (\varepsilon_{nk} - \bar{\mu})^\ell (f_{nk,L}^{(0)} - f_{nk,R}^{(0)}) dk. \quad (2)$$

Using $\mu_L + eV = \mu_R \equiv \mu$, $f_{nk,L}^{(0)} - f_{nk,R}^{(0)} = eV f_{nk}^{(0)'}$, and $\bar{\mu} \rightarrow \mu = \mu_L = \mu_R$ in the limit $V \rightarrow 0$, where V is the infinitesimal voltage difference between the left- and the right-hand 2DEGs, we find

$$Q^{(\ell)} = \frac{2eV(-e)^{1-\ell}}{\pi} \sum_n \left(\int_{\varepsilon_{n,k=0}}^{\varepsilon_{n,k_1}} + \int_{\varepsilon_{n,k_1}}^{\varepsilon_{n,k_2}} + \dots + \int_{\varepsilon_{n,k^*}}^{\infty} \right) \text{sgn}(v_{nk}) (\varepsilon_{nk} - \mu)^\ell f_{nk}^{(0)'} d\varepsilon_{nk}, \quad (3)$$

where $f_{nk}^{(0)'}$ is the first derivative of the Fermi function $f_{n,k}^{(0)} = f^{(0)}(\varepsilon_{n,k})$ with respect to $\varepsilon_{n,k}$, and the lower limit equals the energy $\varepsilon_{n,k=0}$ at $k = 0$. In equation (3), the energy integration over the range $0 < k < \infty$ is chopped into the sum of the integrations between the successive extremum points ε_{n,k_m} , where $\varepsilon_{n,k}$ is a monotonic function of k and ε_{n,k^*} is the last extremum (minimum) point. Each integration can be carried out analytically for both $\ell = 0, 1$, yielding

$$S = \frac{Q^{(1)}}{TQ^{(0)}} = -\frac{k_B}{eF} \sum_n \sum_\gamma C_{n,\gamma} [\beta(\varepsilon_{n,\gamma} - \mu) f^{(0)}(\varepsilon_{n,\gamma}) + \ln(e^{\beta(\mu - \varepsilon_{n,\gamma})} + 1)], \quad (4)$$

where $\beta = 1/k_B T$ and

$$F = \sum_n \sum_\gamma C_{n,\gamma} f^{(0)}(\varepsilon_{n,\gamma}). \quad (5)$$

Here, γ -summation indicates summing over all the energy-extremum points on each curve n ($-\infty < k < \infty$). The quantity $\varepsilon_{n,\gamma}$ is the extremum energy. For a given curve n , $C_{n,\gamma} = 1$ for a local energy minimum point and $C_{n,\gamma} = -1$ for a local energy maximum point. The quantity F equals the number of pairs of the Fermi points at $T = 0$ and is related to G by $G = 2e^2 F/h$. The result in equation (4) is equivalent to the earlier result obtained for SQWRs with a single minimum point for each energy-dispersion curve [4]. It can also be obtained using an energy-dependent transmission-coefficient approach [4, 8, 9].

The TEP is quantized at $T = 0$ K as $S = -(k_B/e) \ln 2/[G/(2e^2/h)]$ in general at the energy-extremum points $\mu = \varepsilon_{n,\gamma}$ in equation (4), where $G = (2e^2/h)(i + 1/2)$ with $i = 1, 2, \dots$ as obtained earlier by Streda [4]. The peak heights of S and corresponding G values satisfy this relationship approximately even at nonzero temperatures in our numerical results to be displayed later.

In this paper, we study a SQWR and DQWRs illustrated in figure 1. We assume that, for both structures, the channel confinement is given by the parabolic potential energy $V(x) = m^* \omega_x^2 x^2/2$, where m^* is the effective mass. The eigenvalues are given for $B = 0$ by $\varepsilon_{nk} = (n + 1/2)\hbar\omega_x + \hbar^2 k^2/2m^*$ with $n = 0, 1, 2, \dots$. The QW depth and widths for the z confinement are designated as V_0 and L_W , while the width of the centre barrier is given by L_B for DQWRs.

We first consider a SQWR illustrated in figure 1(a) with $B \parallel z$ perpendicular to the channel plane. The eigenvalues are given by $\varepsilon_{nk} = (n + 1/2)\hbar\Omega_x + \hbar^2 k^2/2m^{**}$, where $n = 0, 1, \dots$, $\Omega_x = (\omega_x^2 + \omega_c^2)^{1/2}$, $\omega_c = eB/m^*c$, and $m^{**} = m^*/[1 - (\omega_c/\Omega_x)^2]$ [10]. The effective mass m^{**} becomes heavier as B increases, increasing the density of states. As a result, the sublevels n in figure 1(a) become depopulated successively for increasing B . Figure 2 shows G and S of a SQWR obtained from equation (4) for two temperatures as a function of B when several levels are occupied at $B = 0$. The parameter $\hbar\omega_x$ and the electron density n_{1D} are given in the inset. The result in figure 2(a) is independent of L_W and V_0 under the assumption that only the ground level is occupied in the z direction. The TEP is very small when μ lies away from the edges of the sublevels because the contributions to the heat current $Q^{(1)}$ in equation (3) from above μ ($\varepsilon_{nk} > \mu$) cancels those from below μ ($\varepsilon_{nk} < \mu$). This cancellation does not occur when μ is within the thermal energy $k_B T$ of the sublevel edges, yielding spikes for the TEP just before a level is depopulated at the knees of the quantum steps of G . These spikes broaden as T is raised. This behaviour is similar to the density dependence of the field-free TEP studied earlier [4].

For DQWRs, new interesting effects are obtained when B is in the x direction. The role of B is to displace the energy-dispersion parabolas of one QW relative to those of the other QWs in k space by $\delta k = d/\ell_c^2$, where d is the centre-to-centre distance of the QWs and $\ell_c = \sqrt{\hbar c/eB}$. The two parabolas in the QWs with the same n then anticross at the crossing point due to tunnelling, opening a gap Δ_{SAS} between the symmetric and antisymmetric states at $k = 0$ as shown in figure 1(b) for the ground level $n = 0$. In this case, the eigenvalue ε_{nk} and the magnitude of Δ_{SAS} (i.e., mixing of the wavefunctions in the two QWs) depend on the QW width L_W , barrier width L_B , and the barrier height V_0 and are calculated numerically [6, 11]. The parabolas move away from each other in the k -axis direction as $\delta k \propto B$ increases, pushing the gap through the chemical potential μ . The inset in figure 1(b) shows the relative positions of μ with respect to the gap for three different B values. This level splitting occurs for each n . The levels become depopulated as B increases.

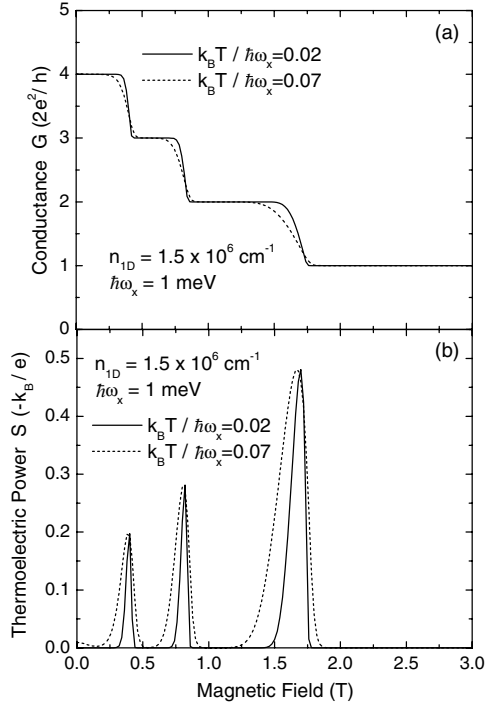


Figure 2. Ballistic (a) G and (b) S for two temperatures in SQWR with three levels occupied initially at $B = 0$. The parameters are defined in the text.

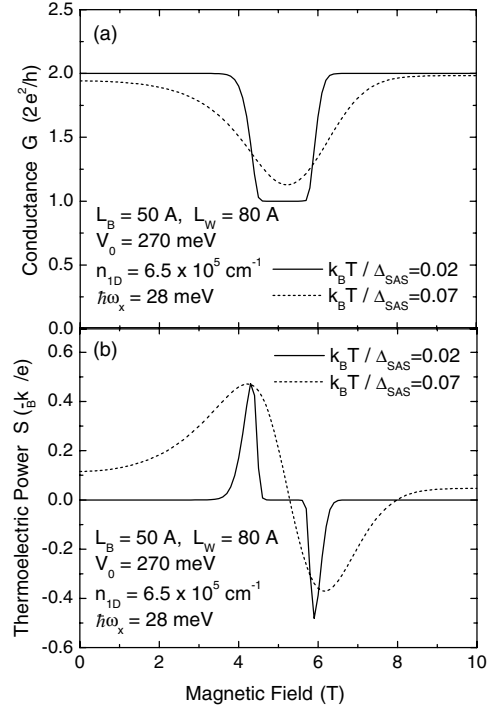


Figure 3. Ballistic (a) G and (b) S for two temperatures in DQWRs with only $n = 0$ occupied. The parameters are defined in the text.

Figure 3 shows S and G calculated from equation (4) for DQWRs at two temperatures for the case of large $\hbar\omega_x$ and low density where only the tunnel-split $n = 0$ doublet is occupied at $B = 0$ as indicated in figure 1(b). The structure parameters are given in the figure. The gap equals $\Delta_{\text{SAS}} = 1.6$ meV for this structure and is insensitive to B . The conductance shows a minimum near $B = 5.1$ T and is V-shaped in striking contrast with the behaviour shown for a SQWR in figure 2(a). The conductance equals the number of pairs of Fermi points in units of $2e^2/h$, namely 2 for $\mu = \mu_1$, 1 for $\mu = \mu_2$, and 2 for $\mu = \mu_3$ in figure 1(b), where the horizontal dotted lines illustrate the fact that the anticrossing gap sweeps through μ as B increases, indicating the positions of the chemical potentials relative to the gap for three concomitant B values: $B_1 < B_2 < B_3$. The TEP shows a surprising feature: it changes sign near the G minimum just before it begins to rise again. At this point, μ crosses the local energy extremum (i.e., maximum) point marked by the hollow circle on the lower branch in figure 1(b), doubling the number of Fermi points and thus G . The dispersion is holelike (i.e., inverted) at this point, yielding a sign reversal for S .

For small $\hbar\omega_x \ll \Delta_{\text{SAS}}$ corresponding to wide channels, many levels are occupied in high-density DQWRs. In this case, G follows a V-shaped dependence on B as shown in figure 4 at two temperatures. A similar B dependence was observed earlier in DQWRs [12]. The inset illustrates the tunnel-split sublevels for this case at B near the G minimum. The B dependence of G can be explained in a similar way as in figure 3(a) by accounting for the Fermi points from all the levels n together with the B -dependent movement of μ with respect to the gap [7]. For SQWRs, G decreases stepwise monotonically as a function of B as in

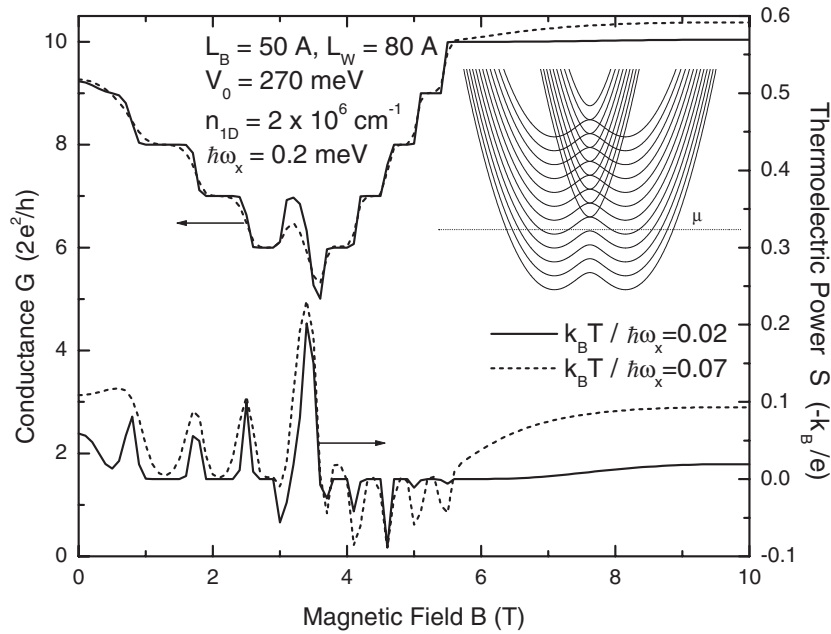


Figure 4. Ballistic G (left axis, upper curves) and S_d (right axis, lower curves) for two temperatures in DQWRs with many levels occupied. The parameters are defined in the text. The inset shows the tunnel-split energy dispersion at $B = 3.4$ T near the G minimum.

figure 2(a) and is not shown [2]. Ballistic S is also displayed for the DQWRs in figure 4 at two temperatures. Note that $-S$ shows positive peaks initially when μ crosses the bottoms of the upper branches successively for lower n values. It changes sign near the G minimum just before it begins to rise again. At this point, μ crosses the local energy maximum point at the top (at $k = 0$) of the lower branch, increasing the number of the Fermi points and thus G . For this point, the dispersion is holelike, yielding the sign reversal for S . From this point on, μ keeps crossing similar local energy maximum points belonging to lower n values, producing successive negative holelike peaks for $-S$. The $-S$ peak near the G minimum at 3.4 T is large because $-S$ is inversely proportional to G .

In summary, we have studied the electron-diffusion thermoelectric power for a general one-dimensional band structure in the ballistic regime. The result was applied to a single-quantum-well channel and tunnel-coupled double-quantum-well channels in a perpendicular magnetic field. In double-quantum-well channels, we showed a field-induced sign reversal and oscillations of the thermoelectric power.

Acknowledgment

Sandia is a multiprogramme laboratory operated by Sandia Corporation, a Lockheed Martin Company, for the US DOE under contract No DE-AC04-94AL85000.

References

- [1] Beenaker C V J and van Houten H 1991 *Semiconductor Heterostructures and Nanostructures (Solid State Physics vol 44)* ed H Ehrenreich and D Turnbull (New York: Academic) and references therein

-
- [2] van Wees B J *et al* 1988 *Phys. Rev. B* **38** 3625
 - [3] van Houten H *et al* 1992 *Semicond. Sci. Technol.* **7** B215
 - [4] Streda P 1989 *J. Phys.: Condens. Matter* **1** L1025
 - [5] Tsaousidou M and Butcher P N 1997 *Phys. Rev. B* **56** R10004
 - [6] Lyo S K 1994 *Phys. Rev. B* **50** R4965
 - [7] Lyo S K 1999 *Phys. Rev. B* **60** 7732
 - [8] Landauer R 1987 *Z. Phys. B* **68** 217
 - [9] Büttiker M 1986 *Phys. Rev. Lett.* **57** 1761
 - [10] Berggren K F *et al* 1988 *Phys. Rev. B* **37** 10118
 - [11] Lyo S K and Huang D H 2001 *Phys. Rev. B* **64** 115320
 - [12] Moon J S *et al* 1999 *Phys. Rev. B* **60** 11530